A humeral coordinate system for in vivo 3-D kinematics of the Glenohumeral joint

Hippolite O. Amadi, Addie Majed, Roger J. H. Emery and Anthony M. J. Bull
Department of Bioengineering and Division of Surgery, Imperial College London, United Kingdom

Summary

The aim of this study was to define axes from clearly identifiable landmarks on the proximal aspect of the humerus and to compare these for reasonable best alternatives to the use of the humeral canal and elbow epicondylar axes to define a humeral coordinate frame (HCF). The elbow epicondylar axis (**EC**) and six different humeral canal axes (**HC**) based on varying lengths of humerus were quantified from twenty-one computed tomography scans of humeri. Six additional axes were defined using the proximal humerus only. These included a line from the centre of a sphere fit on the humeral head to the surface area centroid of the greater tubercle region, (**GT**). The inclinations of these axes relative to **EC** were calculated. **GT** was found to be the most closely aligned to **EC** (13.4° ±6.8°). The inclinations of the other axes ranged from 36.3° to 86.8°. The **HC** axis orientation was found to be insensitive to humeral shaft lengths (variability, within average: 0.6°). This was chosen as 1 of 2 axes for the HCF. This was also the most inter-subject related axis to **EC** with inclination standard deviation of ±1.8°. **EC** was therefore predicted from this such that if the superior axis [1 0 0] of an image scan is maintained and the humerus rotated to make its quantified **HC** align superiorly in the direction [0.98 0.01 0.01], then its **EC** axis lies laterally in the direction [0 0 1]. This study demonstrates that it is possible with confidence to apply an orthogonal coordinate frame to the humerus based on proximal imaging data only.

Key words humeral long axis; epicondylar axis; coordinate frame

Correspondence: Dr Anthony M. J. Bull, Department of Bioengineering, Imperial College London South Kensington Campus, London SW7 2AZ, UK. T: +44 20 75945186; E: a.bull@imperial.ac.uk

Introduction

The osteological anatomy of the proximal humerus is known to vary in terms of the sphericity of the humeral head, (Soslowsky et al. 1992) the position of the bicipital groove (Robertson et al. 2000) and other features (Pearl, 2005; Amadi et al. 2008b). The most robust methods for defining a coordinate frame on the humerus require the use of the distal humerus to define a medio-lateral axis; the use of the proximal humerus only to define a robust coordinate frame has not been proven as yet. The primary need for defining a coordinate frame in this context is to have an approach that can be used for glenohumeral (GH) kinematics studies. The most common axes that are used to define a coordinate frame are the humeral canal (**HC**) and epicondylar (**EC**) axes (Wu et al. 2005; Van der Helm, 1997; Fung et al. 2001; Levasseur et al. 2006; Doyle et al. 1998; Macdonald et al. 2008). Their near-orthogonality gives them mathematical advantages as appropriate axes for the definition of the humeral coordinate frame (HCF), especially when obtained from 2D radiographic images. A number of different techniques have been used in the literature to quantify these axes (Van der Helm, 1997; Wu et al. 2005; Bobrowitsch et al. 2007; Hill, 2006; Amadi, 2006) and their applicability is related to the ease of obtaining the landmarks that have been used to define them. One of the key specifications of these coordinate frames is that landmarks must be chosen such that the resulting principal axes of the coordinate frame automatically orient to “the standard anatomical planes (coronal, sagittal, axial) of a person standing in the upright position” (Amadi et al. 2008a). In the anatomical position, the shaft axis is approximately directed inferior-superiorly while the epicondylar axis is in the approximate medio-lateral sense (De Wilde et al. 2003). Therefore, the commonly used axes satisfy this specification. However, if a scanning field of view (FOV) does not include the distal humeral epicondyles, as is the case in standard shoulder or

chest scans, then the standard coordinate frame definition is not possible. The aims of this study were to:

(i) identify the most closely oriented or consistent related axis to **EC** for its replacement or prediction from a 3D scan of the proximal humerus,

(ii) use the above and a proximal humeral canal axis to propose a HCF definition that can be applied to a standard shoulder scan.

Materials and Methods

Twenty-one CT scans of whole humeri were obtained for this study including two contra-laterals, slice thickness (1.5 mm). An inferior-superior axis through the centre of the humeral shaft was quantified (**HC**) on all the datasets as follows (Figure 1):

- The surgical neck was identified. By anatomical definition, this is the constriction of the humerus immediately distal to the lesser and greater tubercle regions (Gray, 2000). Therefore the immediate axial slice distal to the tubercles was identified as the surgical neck slice.
- The cross-sections of the humeral shaft axial slices within 10 mm distal to the surgical neck slice were identified and contours drawn on these.
- Ellipses were fitted to the humeral shaft at each cross section
- A least-squares line was fitted to the centres of the ellipses.
- This procedure was repeated for each specimen for humeral shaft lengths of 20, 30, 40, 50 and 60 mm distal to the surgical neck (Bobrowitsch et al. 2007, Figure 1).

A sphere-fitting algorithm (Eberly, 2008; Amadi, 2006) was used to define the centre (**c**) of the humeral head (Figure 2). **EC** was defined as a unit vector from the medial margin to the lateral margin of the epicondyles and was found by digitisation of these

marginal regions and quantification of their surface centroids. Five additional proximal humeral axes were quantified on each dataset. These were:

(1) A perpendicular line, **CN** from **c** to **HC**-axis.

(2) **FC**, from **c** to the proximal end-point of the bicipital groove, the fovea capitis, 'f'.

(3) **GT**, from **c** to the area centroid of the greater tubercle region.

(4) **LT,** from **c** to the area centroid of the lesser tubercle region.

(5) **AN**, the normal to the plane upon which the anatomical neck lies (Figure 2).

EC was then compared to all six other quantified axes from the same specimen and the inclinations computed. These were averaged over the twenty-one specimens studied. A coordinate system converter algorithm was applied to **EC** from the specimens expressing and aligning them in a common coordinate system (Amadi et al. 2008b). This also converted the axis with the lowest standard deviation (SD) of inclination to the same common coordinate system and the average of its relative orientation from **EC** was quantified. These were used to define the transfer function for the prediction of **EC** from the proximal aspect of any humerus. Error analysis for the prediction accuracy of the transfer function was carried out by the quantification of the 'Mean Percentage Prediction Error (MPPE)' and the 'Mean Absolute Percentage Prediction Error' (Yaffee and McGee, 2000).

The most appropriate proximal axis to replace **EC** in the new frame definition was considered. This was the second (**$H2_{temp}$**) of the two HCF parenting axes, the first being **HC**. The strengths of inter-subject relationship (inclination SD) between **HC** and the rest of the quantified proximal axes were calculated. **EC** was replaced with its most closely oriented axis provided this had a stronger inter-subject relationship

with **HC** compared with the strongest **EC** relationships. If this condition was not met, **EC** was predicted using the axis of its strongest relationship.

The HCF: The superiorly directed **HC** was 1 of 3 principal axes of the proposed HCF. The cross product between **HC** and $\mathbf{H2_{temp}}$ was quantified as the second orthogonal (**H3**) of the frame. This is directed anteriorly. The third orthogonal axis (**H2**) was quantified as the cross product between **HC** and **H3**. This was approximately in same sense as $\mathbf{H2_{temp}}$.

Results

The average orientation variation of axis **HC** for different humeral shaft lengths was 0.6°± 0.3°. The strongest landmark inter-subject relationship measured by SD of ±1.8° was between **EC** and **HC** (Table 1). An axis directed from the humeral head centre to the area centroid of the greater tubercle (**GT**) was the closest orientation to the epicondylar axis, having the lowest average inclination angle of 13.4° ± 6.8°. **GT** however inclines at an average of 83° and has a relatively weaker landmark relationship of ±3.5° with **HC**. The EC-axis prediction transfer function reveals that if any image data is mapped into a coordinate system such that

- the superior axis [1 0 0] of this system is made to align with that of the original scan coordinate system but
- the humerus rotated to allow the quantified **HC** to align superiorly in the direction [0.98 0.01 0.01] and the normal from **HC** to the greater tubercle centriod in the direction [0.00 -0.02 0.98], then
- the **EC** of such a specimen would lay laterally in the direction [0 0 1].

Error analysis of the transfer function accuracy in the prediction of **EC** from **HC**-axis quantified a ‘mean percent prediction error’ of -0.03% of their inclination angle and a ‘mean absolute percent prediction error’ of 1.6%.

Discussion

At the anatomical position, with the forearm by the side of the body and the palm of the hand facing forward, De Wilde et al (2003) reported that the **EC** inclines at 3° frontal to the coronal plane. In this study, we have shown that the **GT**-axis is nearly in the same direction as the **EC** and may serve as a replacement. However, from our inclination and relationship strength analyses, **EC** is more strongly related (±1.8°) and nearly orthogonal (86.8°) to axis **HC** than **GT** to **HC** (±3.5°, 83°). Therefore **HC** axis quantified by the technique used here and the **EC** axis predicted from this are the best for a consistent HCF. We also quantified the average vectorial relationship between **HC** and **EC** as a transfer-function for the prediction of **EC** of any bone when its axis **HC** is quantified (Amadi et al. 2008b). Hence, if any image data is mapped into a coordinate system with its scan coordinate superior axis [1 0 0] aligned and fixed but the humerus rotated such that its quantified **HC** aligns superiorly in the direction [0.98 0.01 0.01], then axis **EC** of such a specimen lies laterally in the direction [0 0 1]. In addition to a high orientation consistency of **HC** from any available length of humeral shaft and its strong anatomical landmark relationship with **EC**, our error analysis shows that **EC** could be accurately predicted from the quantified transfer function with a mean confidence of 99.97%. The coordinate frame developed in this study can be applied in a further study to define a joint coordinate system for the investigation of the kinematics of the glenohumeral joint.

Authors’ contributions

Hippolite O. Amadi: Contributed to concept/design, extraction of landmarks from data, data analysis/interpretation, drafting of the manuscript, critical revision of the manuscript and approval of the article.

Addie Majed: Contributed to concept/design, medical image acquisition, drafting of the manuscript, critical revision of the manuscript and approval of the article.

Roger J. H. Emery: Contributed to concept/design, medical image acquisition, drafting of the manuscript, critical revision of the manuscript and approval of the article.

Anthony M. J. Bull: Contributed to concept/design, medical image acquisition, extraction of landmarks from data, drafting of the manuscript, critical revision of the manuscript and approval of the article.

References

Amadi HO (2006) Glenohumeral joint kinematics and ligament loading. *PhD Thesis*. Imperial College, University of London, United Kingdom.

Amadi HO, Hansen UN, Wallace AL, Bull AMJ (2008a) A scapular coordinate frame for clinical and kinematic analyses. *J Biomech* **41**, 2144-2149.

Amadi HO, Sanghavi S, Kamineni S, Hansen UN, Bull AMJ (2008b) Definition of the Capsular Insertion Plane on the Proximal Humerus. *J Anat* **212**, 863-867.

Bobrowitsch E, Imhausera C, Graichenb H, Durselen L (2007) Evaluation of a 3D object registration method for analysis of humeral kinematics. *J Biomech* **40**, 511–518.

De Wilde LF, Berghs BM, VandeVyver F, Schepens A, Verdonk RC (2003) Glenohumeral relationship in the transverse plane of the body. *J Shoulder Elbow Surg* **12**, 260-267.

Doyle AJ, Burks RT (1998) Comparison of humeral head retroversion with the humeral axis/biceps groove relationship: A study in live subjects and cadavers. *J Shoulder Elbow Surg* **7**, 456-457.

Eberly D (2008) Least squares fitting data, pp. 6-7. Geometric Tools LLC; http://www.geometrictools.com/Documentation/LeastSquaresFitting.pdf (accessed: 20th February 2009)

Fung M, Kato S, Barrance PJ, Elias JJ, McFarland EG, Nobuhara K, Chao EY (2001) Scapular and clavicular kinematics during humeral elevation: A study with cadavers. *J Shoulder Elbow Surg* **10**, 278-285.

Gray H (2000) The Humerus: In *Lewis WH edited, Anatomy of the human body*, 20th ed online, II.6.a.3. Bertleby.com, NY, USA. http://www.bartleby.com/107/ (accessed: 20th February 2009)

Hill AM (2006) Passive stability of the glenohumeral joint. *PhD Thesis*. Imperial College, University of London, United Kingdom.

Levasseur A, Tetreault P, de Guise J, Nuno N, Hagemeister N (2007) The effect of axis alignment on shoulder joint kinematics analysis during arm abduction. *Clinical Biomechanics* **22**, 758-766.

McDonald CP, Beaton BJ, King GJ, Peters TM, Johnson JA (2008) The effect of anatomic landmark selection of the distal humerus on registration accuracy in computer-assisted elbow surgery. *J Shoulder Elbow Surg* **17**, 833-843.

Pearl ML (2005) Proximal humeral anatomy in shoulder arthroplasty: Implications for prosthetic design and surgical technique. *J Shoulder Elbow Surg* **14,** S99-S104.

Robertson DD, Yuan J, Bigliani LU, Flatow EL, Yamaguchi K (2000) Three-dimensional analysis of the proximal part of the humerus: Relavance to arthroplasty. *J Bone Joint Surg* **82,** 1594-1602.

Soslowsky LJ, Flatow EL, Bigliani LU, Mow VC (1992a) Articular geometry of the glenohumeral joint. *Clin Orthop* **285**, 181-190.

Van der Helm FCT (1997) A standardized protocol for motion recordings of the shoulder. In Veeger HEJ, Van der Helm FCT, Rozing PM, editors. *Proceedings of the First Conference of the International Shoulder Group*. Maastricht, Netherlands.

Wu G, van der Helm FCT, Veeger HEJ, Makhsous M, Roy PV, Anglin C, Nagels J, Karduna AR, McQuade K, Wang X, Werner FW, Buchholz B (2005) ISB recommendation on the definitions of joint coordinate systems of various joints for the reporting of human joint motion-Part II:shoulder, elbow, wrist and hand. *J Biomech* **38**, 981-992.

Yaffee RA, McGee M (2000) Metadiagnosis: In *Introduction to time series analysis and forecasting*, pp. 217–220. Academic Press Inc, San Diego, CA.

Tables

Table 1: Axes inclinations relative to epicondylar and humeral canal axes.

Axes	Inclinations (°)			
	With EC		With HC	
	(mean)	(SD)	(mean)	(SD)
AN	49.8	7.2	52.3	5.0
FC	72.3	6.4	41.0	6.5
GT	**13.4**	6.8	83.0	3.5
CN	36.3	17.4	product	
LT	81.2	7.7	82.8	6.0
HC	86.8	**1.8**	NA	
EC	NA		86.8	**1.8**

Figure Legends

Figure 1: (A) Segmented humeral shaft cross-sections
(B) Humeral head centre and canal axis

Figure 2: Various quantified axes on the humerus

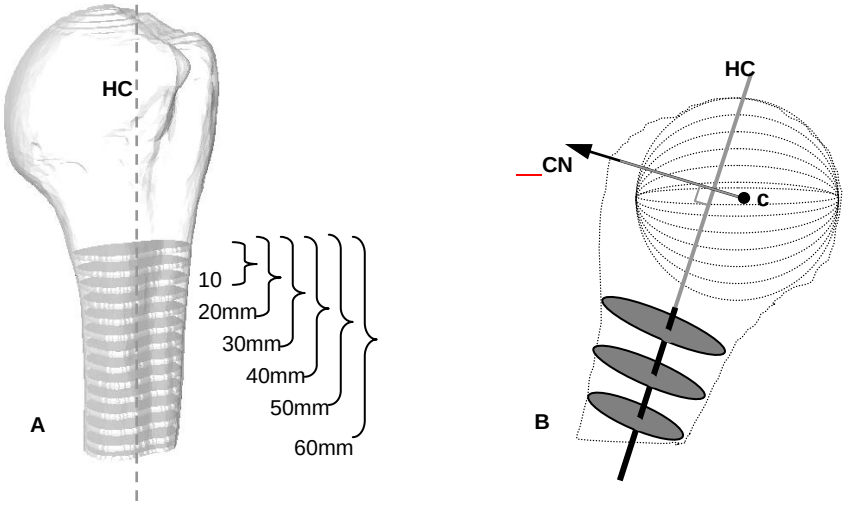

Figure 1: (A) Segmented humeral shaft cross-sections
(B) Humeral head centre and canal axis

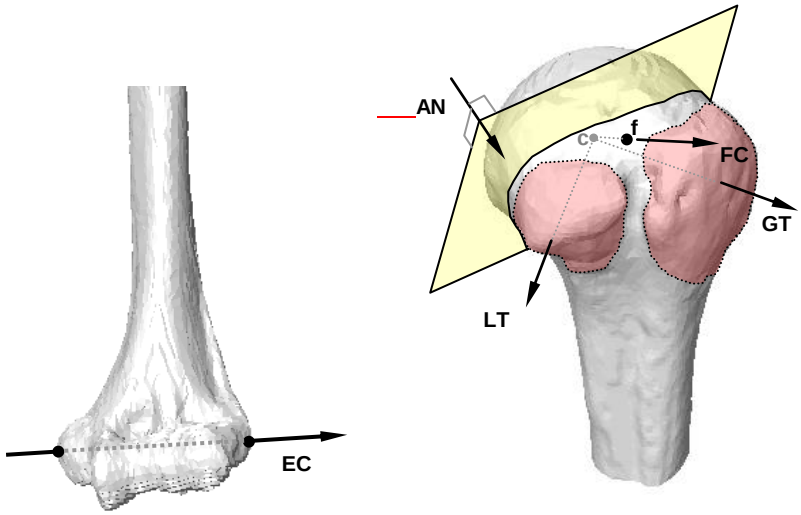

Figure 2: Various quantified axes on the humerus